Hindawi
Geofluids
Volume 2022, Article ID 7332182, 9 pages
https://doi.org/10.1155/2022/7332182

Research Article

Disastrous Mechanism of Water Burst by Karst Roof Channel in Rocky Desertification Mining Area in Southwest China

Jie Suo,[1] Qirong Qin,[1] Wenqiang Wang,[2,3] Zhenhua Li,[2,3] Cunhan Huang,[2,3] Youlin Xu,[4] and Zuguo Chen[5]

[1]*School of Geoscience and Technology, Southwest Petroleum University, Chengdu, 610500 Sichuan, China*
[2]*School of Energy Science and Engineering, Henan Polytechnic University, Jiaozuo, 454000 Henan, China*
[3]*Collaborative Innovation Center of Coal Work Safety and Clean High Efficiency Utilization, Jiaozuo, 454000 Henan, China*
[4]*Institute of Mining Engineering, Guizhou Institute of Technology, Guiyang, 550003 Guizhou, China*
[5]*Xintian Coal Mine, Yonggui Energy Development Co., Ltd., Qianxi, 551500 Guizhou, China*

Correspondence should be addressed to Zhenhua Li; jzlizhenh@163.com

Received 22 April 2021; Revised 7 February 2022; Accepted 5 March 2022; Published 18 March 2022

Academic Editor: Jia Liu

With the development of coal mining in rocky desertification mining area in Southwest China, water burst is becoming an important disaster in coal mine. In order to grasp the evolution characteristics of water gushing channels in coal mining in rocky desertification mining area, the 1402 working face in Xintian Coal Mine is taken as the research object, and the occurrence of aquifers on the roof of the working face is analyzed, and the water filling path of the aquifers is explored. Besides, the evolution characteristics of water passage in coal seam mining are comprehensively analyzed, by the methods of physical similarity simulation, numerical simulation, and microseismic monitoring. The results show that the key water resource is the atmospheric precipitation, which enters the mine through the original karst fissure and mining-induced fissure. With the continuous advance of working face, the fracture height of overburden increases gradually. Specifically, when the advancement distance of working face exceeds 135 m, the water-conducting cracks in the overlying strata develop to the bottom boundary of the Yulongshan limestone aquifer, and then, the mining-induced fracture and aquifer are conducted; when the working face advances 190 m, the overall overburden mining fissure is divided into fissure opening zone and fissure closed zone. Meanwhile, most of the microseismic events occur in the middle part of the karst roof, and the maximum height of microseismic event is 40 m away from the bottom boundary of the Yulongshan limestone, during the advancing process of the working face. When the mining fissure is connected with the original karst fissure, atmospheric precipitation enters the aquifer through the original karst fissure and enters the gob of working face through the mining fissure. The research results provide the references for prediction and prevention for the water burst disaster in rocky desertification mining area in Southwest China.

1. Introduction

As one of the most important coal bases in Southwest China, Guizhou is known as the "Southwest Coal Sea" [1, 2]. At the same time, it is also the largest and most concentrated area of karst distribution in China. The exposed area of limestone reaches 73% of the total area of the province [3, 4]. The underground karst fissures are highly developed in this area. Most of the atmospheric rainfall are not stored on the surface, which flows into the underground karst aquifer [5]. When mining coal seams in karst mining areas, roof karst water seriously threatens the safe and efficient mining of coal in mines [6, 7]. Therefore, it is of great significance to study the evolution characteristics of water gushing channels in karst roof of mining areas, which is beneficial for guiding coal mining in rocky desertification mining area in Southwest China.

Many scholars at home and abroad have done lots of research work on the development height and characteristics of the water-conducting fracture zone in the karst coal roof.

In terms of the development characteristics and laws of the water-conducting fractured zone, researchers represented by Liu Tianquan [8] have summarized and obtained the empirical formula for the development height of the water-conducting fractured zone through years of field research and analysis; Qiao et al. [9] systematically summarized the research progress of aerosol water from four aspects, namely, the formation mechanism of roof aerosol water, disaster-causing mechanism, water disaster prediction and early warning, and key prevention and control technologies; Yang and Xu [10] comprehensively employed the methods of theoretical analysis, similar material tests, and numerical simulation to obtain the evolution law of the water-conducting fracture zone in a large mining height face; Lai et al. [11] used physical similar material simulation experiments, combined with the total station and borehole peep monitoring, 3DEC, and SPSS statistical analysis software, and obtained the migration law of overlying strata in coal seam mining, the development and evolution of fractures, and the distribution characteristics of water-conducting fracture zones; Zou et al. [12] used FLAC3D software to calculate and analyze the plastic failure zone, displacement field, and stress field distribution characteristics of the surrounding rock above the stope before and after the fully mechanized caving work passes the fault and obtained the formation mechanism of the water channel; Wang et al. [13] used theoretical analysis and field detection to obtain the characteristics of the development height of roof water-conducting fractures under the influence of the key layer structure with the mining thickness, and the development height is affected by both the mining thickness and the key layer structure; Zhang et al. [14–16] used the theory of elastic foundation beams to establish a mechanical analysis model for the height of the overburden water-conducting fissure zone of the block-filled stope; Zhu et al. [17] built a coal seam mining model in the karst cave area and obtained the development characteristics of roof mining cracks during coal seam mining; Wang et al. [18] used similarity simulation and theoretical analysis to propose a composite mechanism model of "elastic thin plate" and "parallel pressure arch" for the migration of overlying strata in high-strength mining under three-dimensional spatial conditions; Liu et al. [19] used the borehole television system and borehole simple hydrological observation method, combined with similarity simulation and numerical simulation, and obtained the development characteristics of the overlying water-conducting fissure zone in fully mechanized caving mining in deep and extra-thick coal seams. In terms of the height of the water-conducting fissure zone, Y. P. Zhang et al. [20] used a combination of field measurement, numerical simulation, and similarity simulation to obtain the overburden failure height of the deep thick coal seam in the west of Mongolia with the large mining height; Guo et al. [21] used the method of on-site ground drilling flushing fluid leakage and theoretical analysis methods to obtain the height of the water-transmitting fracture zone in top coal mining under soft and hard alternate overburden conditions; Yang et al. [22] comprehensively used downhole borehole water injection loss observation, borehole television, and numerical simulation technology to obtain the development height of water-conducting fracture zone in fully mechanized caving mining under thick loose layer and weak overburden. In terms of water flow height prediction, Shi et al. [23, 24] combined principal component analysis (PCA), genetic algorithm (GA), and optimized Elman neural network to establish PCA-GA-Elman for the height prediction of water flow fracture zone development. Based on neural network algorithms, Z. H. Li et al. [25] selected mining thickness, mining depth, working face inclination length, coal seam inclination, and overlying rock structure characteristics as the main influencing factors for the height of the water-conducting fissure zone. Based on the particle swarm (POS)-support vector regression (SVR) research method, Xue et al. [26] constructed the Ordos Basin Jurassic coal field water-transmitting fractured zone height prediction model.

The above research results have an important guiding significance for coal mining under water bodies, but there are few studies on the development height and development rules of water-conducting fissures in karst mining areas [27, 28]. This paper employs a combination of theoretical analysis, similarity simulation, numerical simulation, and field microseismic monitoring to analyze the source and volume of water inrush from coal seam mining in karst areas. Through similarity simulation and numerical simulation, the process of connection between the water conduction fissures and the original karst fissures is proved, and the water inrush model for coal seam mining in karst areas is proposed, and the coal seam mining in karst mining areas is mastered. Therefore, the evolution characteristics of roof water gushing channels provide an important reference for safe and efficient coal mining in rocky desertification mining area in Southwest China.

2. Mining and Hydrogeological Conditions

2.1. Water Source of Mine Water Filling. Xintian Mine is located in Qianxi County, Bijie City, Guizhou Province. This area is a typical karst mining area. Mine water is mainly filled with two major water sources, namely, atmospheric precipitation and underground karst water. Atmospheric precipitation is the main source of replenishment for surface water and underground karst water, which restricts the dynamic changes in the flow of surface rivers and mines. According to the meteorological data provided by the Qianxi County Meteorological Bureau, the annual rainfall in the mining area is about 940~1090 mm, and the rainy season is from May to September, accounting for about 80% of the annual rainfall. Under normal circumstances, atmospheric precipitation mainly replenishes the Yulongshan limestone aquifer through shallow weathering fissures, structural fissures, and sinkholes. Continuous rainfall increases the water supply to the underground Yulongshan limestone aquifer, so atmospheric precipitation is the direct water source for filling water in the shallow limestone aquifer of the mine. When the mining fissure is connected to the aquifer, the aquifer becomes a direct source of water for the mine.

The water richness of the aquifer in the Yulongshan section of the Yelang Formation in the mining area is generally not strong and extremely uneven. However, affected by the structure of the fault and lateral fracture zone, the karst is strongly developed, and the underground karst space is connected with the surface karst, especially during rainfall. Atmospheric precipitation and surface water leak along surface creeks and sinkholes to replenish the ground, resulting in a large amount of groundwater enrichment in the limestone aquifer in the Yulongshan section, which becomes an enrichment zone for groundwater. The lower part contains the limestone of the Changxing Formation with an average thickness of 35 m. Because there is a water barrier in the middle, and the stratum is not exposed, deep buried, and poor replenishment conditions, the limestone of the Changxing Formation is a weak aquifer.

2.2. Mine Water Filling Channel. The water-filled channel in the karst mining area is composed of the original karst fissures and mining fissures, which is different from the water-filled channels in ordinary mining areas only by the mining fissures. The original fissures include weathered zones, faults, collapse pits, sinkholes, and underground karst fissures. Mining fissures are the fractures formed by the collapse of the roof of underground coal mining, forming the water-filling channel of the karst mining area. When the mining fissures and karst fissures are connected, karst water continuously flows into the well, seriously affecting the safe and efficient mining of the working face.

2.3. Overview of Test Working Face. The 1402 working face of Xintian Coal Mine is selected as the test working face, which has a strike length of 147 m and a slope length of 1148 m. The average mining thickness of the coal seam is 3 m, and the average inclination angle is 3°. The working face elevation is +912~+948 m. The working face is located to the north of the three main lanes in the south wing, 1401 mined area on the east, 1404 unmined working face on the west, 1402 bottom extraction lane under 1402 belt transport lane, and original 1# bottom extraction under 1402 track transport lane. The surface is barren hills, and the buried depth is more than 340 m, and the mining has little impact on the ground. The layout of 1402 working face is shown in Figure 1.

3. Similarity Simulation of Evolution Characteristics of Water Gushing Channel

3.1. Model Design and Establishment. According to the mining geological conditions of the 1402 working face, the buried depth of working face is about 340 m, and the mining thickness of the coal seam is only 3 m. In consideration, if the similarity ratio is small, the geometric similarity ratio is selected as 1 : 100; and the length, width, and height of the selected similarity simulation test bench are2500 mm × 200 mm × 1300 mm, and the simulated rock layer height is 120 m. According to similarity simulation principles, the top loading of the model fails to simulate the weight of the rock formation. According to the original model, the loading value is

$$q_p = \frac{P}{F} = \gamma_p(H - H_l). \tag{1}$$

The load value q_m on the model is

$$q_m = \frac{q_p}{C_{\mathrm{L}} \cdot C_\gamma} = \frac{\gamma_P(H - H_1)}{C_{\mathrm{L}} \cdot C_\gamma}, \tag{2}$$

where q_p is the prototype unsimulated rock formation pressure, KPa; H is the mining depth, m; H_1 is the height of the simulated roof rock formation, m; the thickness of the unsimulated overburden is 280 m, where the average bulk density of the overburden is 2800 KN/m^3; and the load q_m applied to the model is 3484 KPa. This load is compensated by the pressure of the hydraulic column on the test bench. Two displacement measuring lines are arranged on the model, a total of 48 displacement measuring points, and each measuring point is 10 cm apart. The 1# measuring line is located at the interface of the limestone top plate of the Changxing Formation, and the 2# measuring line is located at the interface of the limestone floor of the Changxing Formation. In order to eliminate the influence of the boundary, 30 m coal pillars are left on the left and right sides of the model, and the excavation is carried out gradually from right to left, shown in Figure 2.

This experiment uses sand as aggregate, calcium carbonate and gypsum as cementing materials, and borax as retarder. According to the calculation method of the simulated strength value of similarity materials, a reasonable ratio of similarity materials in each layer is obtained. According to the cross-sectional area of the model frame, the thickness of the rock (coal), and the geometric similarity ratio, the weight of the similarity material of each rock (coal) layer is calculated (considering the richness factor of 1.2), and the proportion number and parameters are shown in Table 1.

3.2. Development Characteristics of Water Gushing Channels

3.2.1. Fracture Characteristics of Overlying Strata. The mining method of oblique mining is adopted in the 1402 working face. During the mining process, collapse, subsidence, and layer separation occur in sequence above the gob. When the working face advances to 85 m, the overburden fracture occurs for the fifth cycle. The overburden collapse height is 24 m, and the fracture angle on the side of the working face is 55°, which is smaller than the fracture angle at the open cut. The lower part contains the limestone of the Changxing Formation. There are a large number of separation zones, and the mining cracks do not penetrate the limestone of the Changxing Formation; when the working face advances to 150 m, the overburden fracture occurs in the ninth cycle. The overburden fracture height is 85 m, and the fracture angle on the side of the working face is 56°, and the fracture angle at the open cut is 60°, and the fracture angle between the two fracture lines is 60°. The strata span is 80.6 m, and the mining fissures have fully developed to the top of the

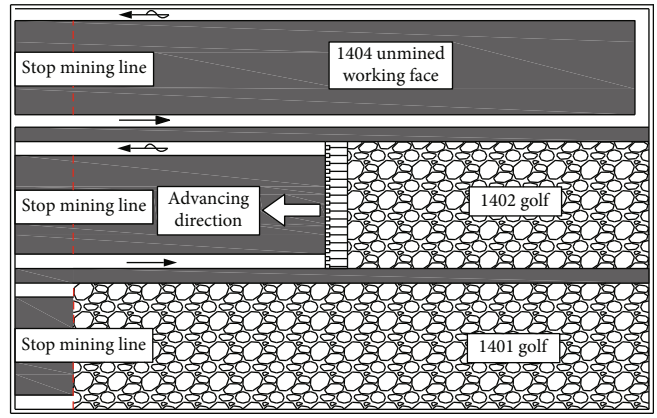

Figure 1: Schematic layout diagram of 1402 working face.

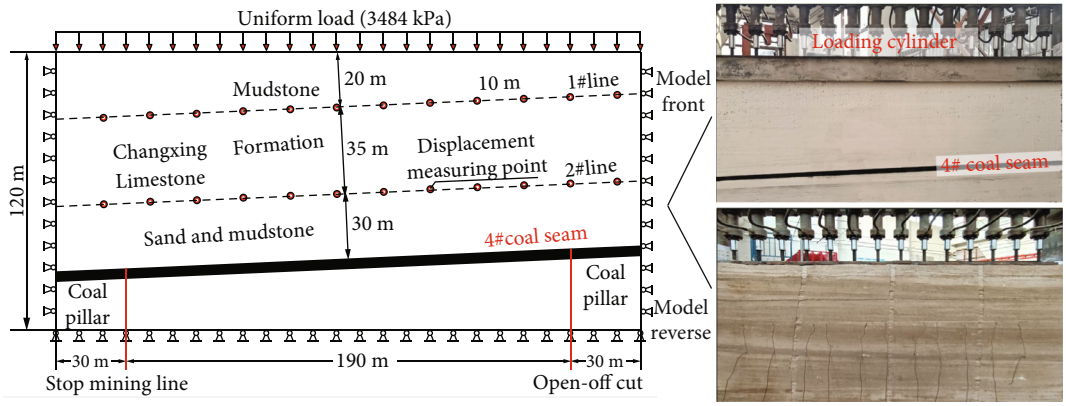

Figure 2: Displacement measuring point arrangement and excavation position.

Table 1: Similarity simulation test ratio and parameters.

No.	Lithology	Thickness (cm)	Matching number	Compressive strength (MPa)	Tensile strength (MPa)	Cohesion (MPa)	Density (g/cm^3)
1	Sand and mudstone	20	655	29.9	2.31	9.91	2.770
2	Limestone	35	437	51.4	5.70	17.12	2.800
3	Sand and mudstone	30	655	29.9	2.31	9.91	2.770
4	4# Coal	3	773	3.9	0.28	1.23	1.461
5	Sand and mudstone	32	655	29.9	2.31	9.91	2.770

model, indicating that the fracture height of the fissures has reached the Yulongshan limestone floor at this time; when the working face advances to 190 m, the overburden fracture occurs for the thirteenth cycle. The fracture angle on the side of the working face is 52°, and the fracture angle at the open cut is 60°, and the strata span between the two fracture lines is 132.6 m. The fractured height of the fissure has reached the inside of Yulongshan limestone. When the 4# coal seam is excavated, there are 13 periodic roof breaks in the overburden. The first break step is 35 m, and the average periodic break step is 11.9 m. The mining fissures are connected to the Yulongshan limestone aquifer, shown in Figure 3.

During the excavation of the working face, the overburden fracture height is recorded. When the working face advances to 95 m, the overburden fracture height is 45 m, and the limestone of the Changxing Formation has been fractured; when the working face advances to 110 m, the Changxing Formation is completely broken; when the working face advances to 135 m, the overburden fracture height is 85 m, indicating that the cracks have developed to the top of the model. Due to the size of the model, with the further excavation of the coal seam, the height of the overburden cracks no longer changes on the model. However, the limestone of the Yulongshan section gradually

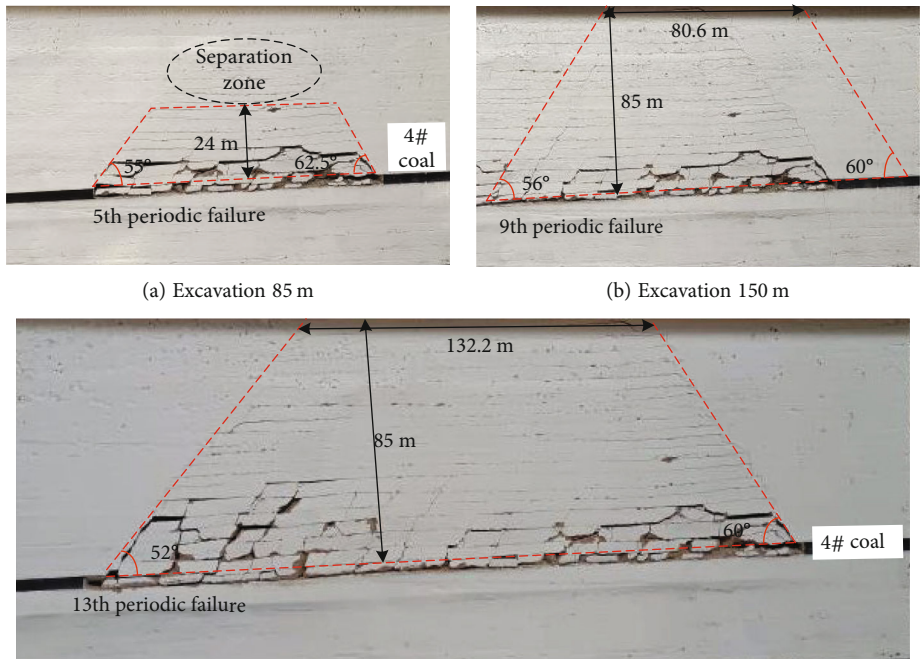

(a) Excavation 85 m

(b) Excavation 150 m

(c) Excavation of 190 m

Figure 3: Periodic weighting of coal seam.

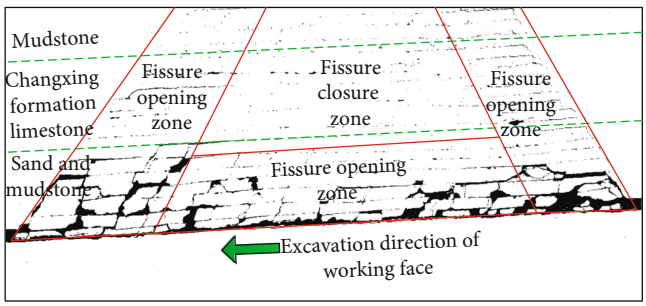

Figure 4: Fissure field in mining 4# coal seam.

breaks in actual conditions, and the mining fissures continue to expand into the limestone of the Yulongshan section.

3.2.2. Displacement of Overlying Rock. The displacement change of the limestone roof in the Changxing Formation during the mining process of the 4# coal seam is obtained. When the working face advances to 110 m, the survey line begins to bend and deform, indicating that the upper part of the Changxing Formation limestone begins to bend and sink; when the working face advances to 120 m, the maximum subsidence value of 1# survey line is -507.3 mm, and the limestone of Changxing Formation breaks and sinks at this time; with the continuous advancement of working face, the displacement curve sinks periodically. After the working face is mined, the maximum sinking value of the 1# survey line is -1006 mm.

The displacement change of the limestone floor in the Changxing Formation during the mining process of the 4# coal seam is obtained. When the working face advances to 85 m, the 2# survey line is bent and deformed. At this time, the limestone floor of the Changxing Formation breaks and sinks. With the continuous advancement of the working face, the floor sand and mudstone layers are periodically broken. When the coal seam is excavated, the maximum subsidence of the 2# survey line is -1332.1 mm.

3.2.3. Fissure Field. The sketch map of the distribution of overburden cracks in the 4# coal seam after mining is shown in Figure 4. The overburden fissure field is divided into fissure opening area and fissure closure area. The opening angle of the overburden rock near the working face and the open cut is relatively large, and the fissures are more developed. The water conductivity is strong, and the upper fissures in the middle of the gob are closed due to compaction, and the water conductivity is poor. After the coal seam is fully mined, the mining fissures have developed to the top of the model and are connected to the Yulongshan limestone aquifer. The roof water enters the gob through mining fissures. Because it is inclined mining, the karst water in the gob flows to the working face, which is consistent with the water gushing phenomenon that occurs in the actual coal seam mining process.

4. Field Measurement of Breaking Height in Overlying Rock

4.1. Layout of Microseismic Monitoring Points. According to the general principle that all measuring points form a spatial body, candidate points for the station layout of the microseismic monitoring system of Xintian Mine have been

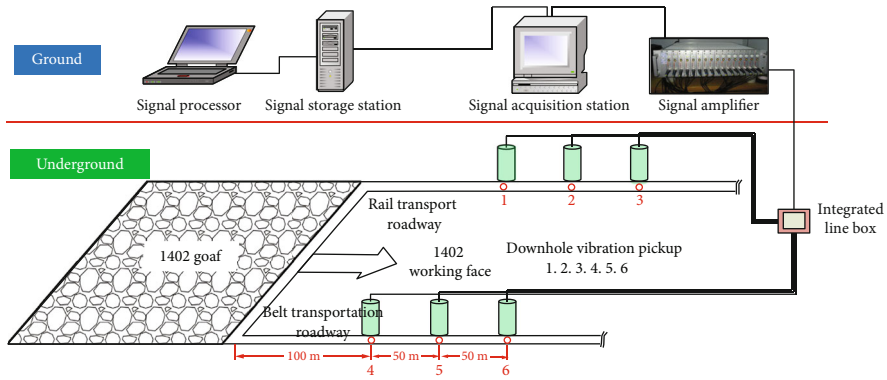

Figure 5: Working principle and schematic diagram of measuring point layout.

Table 2: Optimal plan for measuring point layout.

N0.	Location	Coordinate		
		X	*Y*	*Z*
1	1402 Track roadway	3001528.013	35608039.428	930.590
2	1402 Track roadway	3001547.067	35608007.589	921.339
3	1402 Track roadway	3001569.681	35607977.316	913.300
4	1402 Belt roadway	3001407.313	35607944.994	937.110
5	1402 Belt roadway	3001428.630	35607914.794	931.960
6	1402 Belt roadway	3001452.382	35607880.289	925.357

selected. The schematic diagram of the designed layout of measuring points is shown in Figure 5.

The optimal plan for the location of the measuring point determined by analysis and measurement calculation is shown in Table 2.

4.2. Analysis of Microseismic Monitoring Results. The distribution of microseismic events was monitored from November 11, 2019, to January 5, 2020. The microseismic events mostly occurred in front of the work and were mostly biased towards the 1402 belt lane, and the energy range was in the range of 0~1000 J. There were only four microseismic events in the mined-out area behind the working face, with energy three times greater than 1000 J.

The cross-sectional view of the microseismic event in the track lane at 1402 working face is obtained. The microseismic event gradually decreases in the front of the working face, but the energy of the event increases as it goes up. There are three locations in front of the work where the energy of the microseismic event exceeds 100 J. One of them is the bottom of the Changxing Formation limestone, and the remaining two are located inside the Yulongshan limestone. The two locations are 5 m and 45 m away from the bottom boundary of the Yulongshan rock formation, and the highest point is 125 m from the roof of 4# coal seam.

The section view of the microseismic event at the 1402 working face is obtained. During the monitoring period, the upper rock formations at the 1402 working face have four relatively large vibrations, all with energy greater than 100 J. Moreover, the locations of the incidents are basically near the vertical line of the working face. The positions from bottom to top are as follows: 3 m below the Changxing Formation limestone floor, 1 m below the Yulongshan limestone floor, and 45 m above the Yulongshan limestone floor.

During the monitoring period, microseismic events mostly occur on the leading working face. Large energy events exceeding 100 J are mainly concentrated in the middle of the working face and lagging behind the working face and occur in the upper part of the gob behind the working face. According to the microseismic event profile, the maximum height of the microseismic event is located at the Yulongshan limestone 125 m away from the 4# coal seam. Therefore, the height of the water gushing channel develops to the Yulongshan limestone, and the water gushing channel is connected to the Yulongshan limestone cave.

5. Analysis of Mine Water Inflow Process

After the working face is fully recovered, there is continuous water gushing to the working face behind the working face. Temporary water pumps are installed on the working face to pump the water to the storage tank of the stop line. After the precipitation, it is discharged into the underground silo through the water pump, shown in Figure 6.

5.1. Analysis of Mine Water Inflow. By analyzing the average monthly water inflow from April 2015 to October 2019 and the atmospheric rainfall data in the area, the relationship between atmospheric rainfall and mine water inflow is obtained, shown in Figure 7. The change in mine water inflow is closely related to atmospheric rainfall, indicating that there is a water inflow channel between the mine and the ground, resulting in an increase in mine water inflow after atmospheric rainfall.

5.2. Mine Water Gushing Process. Based on the hydrogeological conditions of the mining area, a conceptual model of karst roof gushing water is proposed, shown in Figure 8. There are many bead-shaped sinkholes on the surface. The limestone karst fissures in the upper part of the Yulongshan section are relatively developed, and the karst fissures in the lower part are poorly developed. Gas and rain tend to enter underground karst caves and karst fissures through sinkholes and surface karst cracks, becoming a potential threat to coal mining. Xintian Coal Mine mainly mines the 4# and 9# coal seams. With the increase of the mining space

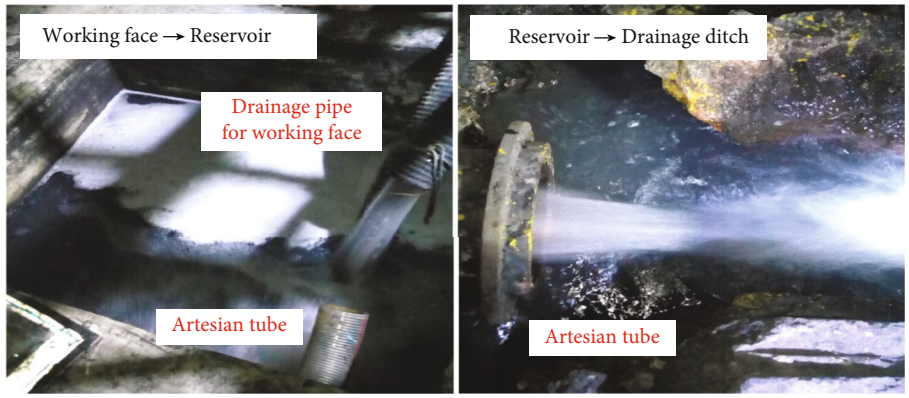

Figure 6: Underground gushing and drainage situation.

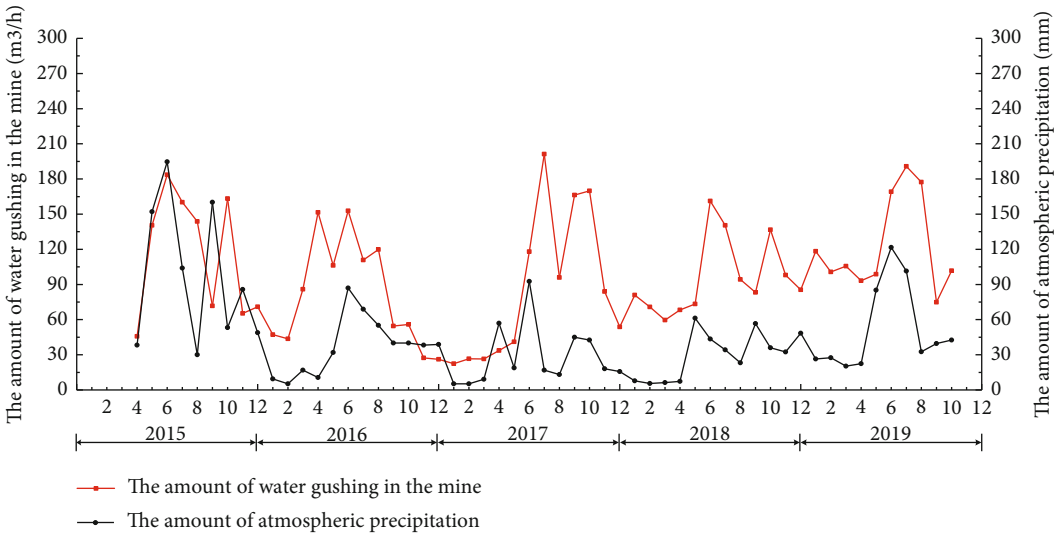

Figure 7: The relationship between mine water inflow and atmospheric rainfall in Xintian Mine.

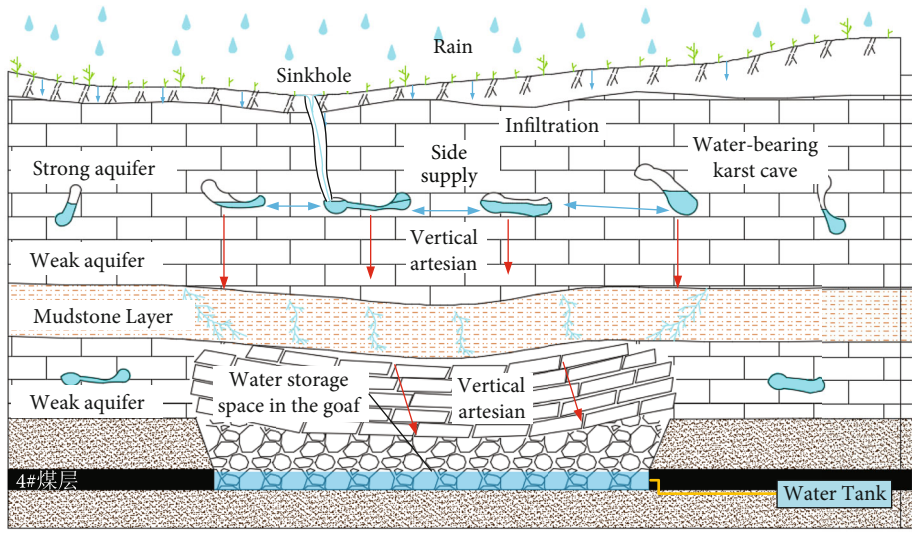

Figure 8: Conceptual model of water inrush from karst roof in coal mining.

of the 4# coal seam, the mining fissures gradually develop upwards, and the original fissures further develop and expand under the influence of mining.

When the distance between the coal seam and the aquifer reaches the critical value of water gushing, the original karst fissures and mining fissures are connected to form a water gushing channel between the surface-karst cave-working face or gob. When 4# coal seam is mined in Xintian Mine, the working face is threatened by roof karst water, and the mining work of 9# coal seam is also threatened by roof karst water.

6. Conclusion

(1) Atmospheric precipitation in karst areas is the key supply water source for the Yulongshan limestone aquifer, which enters the mine through the original karst fissure and mining-induced fissure. Besides, the Yulongshan limestone aquifer is the direct source of water gushing in the mine

(2) There are ultrahigh-conductivity fracture zones in coal seam mining in karst mining areas. When the working face advances 135 m, the fissure develops to the Yulongshan limestone floor. With the continuous advancement of the working face, the height of the water-conducting fissure zone continues to develop upwards. The final monitoring results show that the development height of water-conducting fissure zone is 125 m

(3) When the 4# coal seam is fully mined, the mining fissure is connected to the karst fissure, and a water gushing channel is formed between the surface, the karst cave, and the working face (or gob). On this basis, a conceptual model of karst roof gushing in coal mining in rocky desertification mining area is proposed

Data Availability

The data used to support the findings of this study are included within the article.

Conflicts of Interest

The authors declare that they have no conflicts of interest.

Acknowledgments

This work was supported by the National Natural Science Foundation of China (52174073, 41972175, and 51774110) and the Natural Science Foundation of Henan Province (222300420007).

References

[1] S. J. Wang, "Discussion on the concept deduction of karst rocky desertification and its scientific connotation," *China Karst*, vol. 2002, no. 2, pp. 31–35, 2002.

[2] Z. W. Liu, M. Q. Zhang, and S. R. Wang, "Catastrophe prediction and treatment technology of karst tunnel," *Second edition, Beijing: Science Press, vol.*, vol. 2007, 2007.

[3] Z. Z. Cao, Y. L. Ren, Q. T. Wang, B. H. Yao, and X. C. Zhang, "Evolution mechanism of water-conducting channel of collapse column in karst mining area of Southwest China," *Geofluids*, vol. 2021, 2021.

[4] Y. Xue, J. Liu, P. G. Ranjith, Z. Zhang, F. Gao, and S. Wang, "Experimental investigation on the nonlinear characteristics of energy evolution and failure characteristics of coal under different gas pressures," *Bulletin of Engineering Geology and the Environment*, vol. 81, no. 1, article ???, 2022.

[5] J. Liu, Y. Xue, Q. Zhang, H. Wang, and S. Wang, "Coupled thermo-hydro-mechanical modelling for geothermal doublet system with 3D fractal fracture," *Applied Thermal Engineering*, vol. 200, article 117716, 2022.

[6] P. Hou, Y. Xue, F. Gao et al., "Effect of liquid nitrogen cooling on mechanical characteristics and fracture morphology of layer coal under Brazilian splitting test," *International Journal of Rock Mechanics and Mining Sciences*, vol. 151, p. 105026, 2022.

[7] Y. Xue, J. Liu, P. G. Ranjith, X. Liang, and S. Wang, "Investigation of the influence of gas fracturing on fracturing characteristics of coal mass and gas extraction efficiency based on a multi-physical field model," *Journal of Petroleum Science and Engineering*, vol. 206, article 109018, p. 109018, 2021.

[8] State Coal Industry Bureau, "Coal pillars and coal mining regulations for buildings, water bodies, railways and main shafts," *Beijing: Coal Industry Press*, vol. 2000, no. 1, pp. 225–233, 2000.

[9] W. Qiao, Z. W. Wang, W. P. Li et al., "The formation mechanism, hazard mechanism and prevention technology of coal mine roof separation water damage," *Journal of China Coal Society*, vol. 46, no. 2, pp. 507–522, 2021.

[10] Y. L. Yang and G. G. Xu, "Evolution of water-transmitting fault zone in large mining height working face under Luohe sandstone aquifer," *Coal Mine Safety*, vol. 52, no. 3, pp. 30–35, 2021.

[11] X. P. Lai, X. D. Zhang, P. F. Shan, F. Cui, B. W. Liu, and R. Bai, "Development law of water-conducting cracks in overlying strata in mining of three-soft coal seams under thick loose layers," *Chinese Journal of Rock Mechanics and Engineering*, vol. 40, no. 9, pp. 1739–1750, 2021.

[12] G. H. Zou, C. Zhang, D. Tian et al., "Research on the formation mechanism of the water channel through the overlying strata of the fault group in fully mechanized caving face," *Metals and Minerals*, vol. 539, no. 5, pp. 65–70, 2021.

[13] X. Z. Wang, J. L. Xu, H. K. Han, J. F. Ju, and Y. T. Xing, "Stepped development characteristics of roof water-conducting fissure height with mining thickness," *Journal of China Coal Society*, vol. 44, no. 12, pp. 3740–3749, 2019.

[14] Y. Zhang, S. Cao, T. Wan, and J. Wang, "Field measurement and mechanical analysis of height of the water flowing fracture zone in short-wall block backfill mining beneath the aquifer: a case study in China," *Journal of Mining & Safety Engineering*, vol. 2018, no. 1, pp. 1–12, 2018.

[15] Y. Zhang, S. G. Cao, X. P. Lai et al., "Analysis of the mechanical characteristics of the development of water-transmitting fractures in the overlying rock in short-wall block mining," *Journal of China Coal Society*, vol. 45, no. S2, pp. 551–560, 2020.

[16] Y. Zhang, S. G. Cao, X. P. Lai, C. Z. Zhao, and S. Y. Du, "Research on development mechanism and control of water-conducting fissures in overlying rock in short-wall block-filling mining," *Journal of Mining & Safety Engineering*, vol. 36, no. 6, pp. 1086–1092, 2019.

[17] C. Q. Zhu, D. G. Cui, Z. Zhou, Q. F. Li, and Y. J. Huang, "Similarity simulation of mining fissure development and cave failure characteristics in karst mining area," *Chinese Journal of Underground Space and Engineering*, vol. 15, no. 1, pp. 93–100, 2019.

[18] Y. G. Wang, W. B. Guo, E. H. Bai et al., "Study on the characteristics and mechanism of overlying strata migration in high-strength mining," *Journal of China Coal Society*, vol. 43, no. s1, pp. 28–35, 2018.

[19] Y. F. Liu, S. D. Wang, and X. L. Wang, "Development characteristics of water conducting fracture zone in overlying strata in fully mechanized caving mining in deep and extra-thick coal seam," *Journal of China Coal Society*, vol. 39, no. 10, pp. 1970–1976, 2014.

[20] Y. P. Zhang, Y. G. Zhang, Y. T. Liu, Y. J. Song, and Q. Y. Zhao, "Research on overburden failure height of large-cutting height fully mechanized face in deep thick coal seam in western Mengxi," *China Safety Science Journal*, vol. 30, no. 8, pp. 37–43, 2020.

[21] W. B. Guo, G. Z. Lou, and B. C. Zhao, "Research on the height of water-conducting fracture zone in top coal caving mining with soft and hard overlying strata in Lugou coal mine," *Journal of Mining & Safety Engineering*, vol. 36, no. 3, pp. 519–526, 2019.

[22] D. M. Yang, W. B. Guo, G. B. Zhao, Y. Tan, and W. Q. Yang, "Development height of water-conducting fracture zone in fully mechanized caving mining under thick loose layer and weak overburden," *Journal of China Coal Society*, vol. 44, no. 11, pp. 3308–3316, 2021.

[23] L. Q. Shi, H. B. Wu, Y. L. Li, and W. K. Li, "PCA-GA-Elman optimization model for predicting the development height of water-conducting fracture zone," *Journal of Henan Polytechnic University (Natural Science Edition)*, vol. 40, no. 4, pp. 10–18, 2021.

[24] L. Q. Shi, H. Q. Xin, P. H. Zhai et al., "Study on the calculation of the height of the water conducting fracture zone under the condition of large mining depth," *Journal of China University of Mining and Technology*, vol. 41, no. 1, pp. 37–41, 2012.

[25] Z. H. Li, Y. C. Xu, L. F. Li, and C. Z. Zhai, "Prediction of the height of water conducting fracture zone based on BP neural network," *Journal of Mining & Safety Engineering*, vol. 32, no. 6, pp. 905–910, 2015.

[26] J. K. Xue, H. Wang, C. H. Zhao, J. Yang, Z. F. Zhou, and D. B. Fang, "Prediction of the height of water-transmitting fissure zone and roof water filling mode of Jurassic coalfield in Ordos Basin," *Journal of Mining & Safety Engineering*, vol. 37, no. 6, pp. 1222–1230, 2020.

[27] Y. Xue, J. Liu, X. Liang, S. Wang, and Z. Ma, "Ecological risk assessment of soil and water loss by thermal enhanced methane recovery: numerical study using two-phase flow simulation," *Journal of Cleaner Production*, vol. 334, article 130183, p. 130183, 2022.

[28] Z. Z. Cao, Y. F. Xue, H. Wang, J. R. Chen, and Y. L. Ren, "The non-Darcy characteristics of fault water inrush in karst tunnel based on flow state conversion theory," *Thermal Science*, vol. 25, no. 6, pp. 4415–4421, 2021.